STACKING SEQUENCE OPTIMIZATION USING FRACTAL BRANCH AND BOUND METHOD FOR ASYMMETRICAL COMPOSITE LAMINATES

Ryosuke Matsuzaki*, Akira Todoroki**
***Tokyo Institute of Technology, **Tokyo Institute of Technology**

Keywords: *Stacking Sequence Optimization, Lamination Parameter, Asymmetrical Laminate, Response Surface, Branch and Bound Method, Cylindrical Shell, Buckling.*

Abstract

Fractal branch-and-bound method has been developed by the authors for stacking-sequence optimizations of composite laminates. However, the method was limited to the symmetric and balanced composite laminates.

In the present study, we focus on the stacking-sequence optimizations of all feasible laminates including asymmetrical composite laminates. In the asymmetrical laminates, nine lamination parameters including three coupling-lamination parameters exist, and its feasible design region of fractal pattern is unrevealed. The paper clarifies the feasible region in which the in-plane, out-of-plane and coupling lamination parameters create fractal patterns of tetrahedrons or tetradecahedrons. Using the fractal patterns of lamination parameters, the improved fractal branch-and-bound method is proposed for asymmetrical laminates. This new method is applied to stacking-sequence optimization problems of maximization of buckling load of cylindrical laminated shells. As a result, the method is successfully applied, and a practical optimal stacking-sequence is obtained with low computational cost.

1 Introduction

Since the mechanical properties of composite laminates strongly depend on stacking sequences, stacking-sequence optimizations are indispensable for laminated composite structures. In a practical use, the fiber angles in a laminate are limited to small sets comprise of 0º, ±45º and 90º-plies, because of lack of experimental data or fabrication process efficiency. To comply with this demand, stacking-sequence optimizations become combinatorial optimization problems of selecting a required number of plies of each orientation and determining an optimal stacking-sequence. Combinatorial optimization problems, however, usually require large computational resources.

To solve stacking-sequence optimization problems, genetic algorithms (GAs) are generally used because the GAs are admitted to be effective for combinatorial optimization [1-3]. The GA, however, requires high computational cost because the algorithm repeats evaluations for numerous genes and by generations. To reduce the computational cost for the stacking-sequence optimizations, Todoroki and Haftka [1] employed a response surface for reduction of evaluation cost. This response surface method adopts lamination parameters introduced by Miki [4] and Fukunaga [5] as variables of the response surface. Using lamination parameters, the number of variables is independent of the number of plies, and quadratic polynomials are enough to approximate entire objective function. The GA, however, still requires a large number of adjustments to obtain high performance, and the method cannot always obtain the real optimal stacking-sequence because the method is probabilistic approaches.

Todoroki *et al*. [6-9] has proposed a fractal branch-and-bound method as a deterministic optimization method of stacking sequences based on a well-known branch-and-bound method. This method has been applied to stacking-sequence optimization problems such as maximizing buckling load of a hat-type stiffener [7], and improving flutter limit of composite delta wing [9].

This method, however, is limited to the problems for symmetrical and balanced laminates. The symmetrical and balanced laminates can be approximately treated as orthotropic laminates, which require only two in-plane and two out-of-

plane lamination parameters as design variables. The set of the orthotropic laminates creates two-dimensional fractal patterns when they are plotted in the coordinates of the in-plan and out-of-plane lamination parameters [7]. The symmetrical laminates are widely used as composite panels because coupling stiffness matrix is equal to zero: they do not have coupling stiffness between tension and bending. However, for structures regarded as symmetrical as an entire structure like cylindrical laminated shells or thin walled prismatic columns, the asymmetrical laminates has to be taken into account for the stacking-sequence optimization [10-13]. In addition, asymmetrical laminates are also favored for helicopter blades or fan blades of aircraft engines because the asymmetrical laminates have smart functions owing to coupling effect [14-18]. Although the fractal branch-and-bound method needs to be improved for stacking-sequence optimization of asymmetrical laminates, the detailed feasible fractal pattern of coupling lamination parameters is quite complicated and not revealed.

In the present study, we propose an improved fractal branch-and-bound method, which can be applied to stacking-sequence optimizations of asymmetrical laminates. In asymmetrical laminates, three coupling lamination parameters exit as well as three in-plan and three out-of-plane lamination parameters. We reveal the detailed feasible region of lamination parameters of asymmetrical laminates when the fiber angle is limited to 0°, ±45° and 90°; it indicates that the in-plane and out-of-plane lamination parameters create self-similar fractal patterns of tetrahedrons, and the coupling lamination parameters create that of tetradecahedrons. Using the fractal patterns of in-plane, out-of-plane, and coupling lamination parameters, the improved fractal branch-and-bound method is proposed here. The proposed method is applied to stacking-sequence optimizations of buckling-load maximization of composite cylindrical shells.

2 Stacking Sequence Optimization Method

2.1 Lamination Parameter

In-plane stiffness terms of asymmetrical laminates are represented with in-plane lamination parameters (e.g. Ref. [13]). The in-plane lamination parameters are defined as follows:

$$\boldsymbol{V}^{A}_{[1,2,3.4]^T} = \frac{1}{h}\int_{-\frac{h}{2}}^{\frac{h}{2}} \begin{bmatrix} \cos 2\theta(z) \\ \cos 4\theta(z) \\ \sin 2\theta(z) \\ \sin 4\theta(z) \end{bmatrix} dz = \sum_{k=1}^{N} \left(a_k^A - a_{k-1}^A\right) \begin{bmatrix} \cos 2\theta_k \\ \cos 4\theta_k \\ \sin 2\theta_k \\ \sin 4\theta_k \end{bmatrix} \quad (1)$$

where h is the thickness of laminate, z is coordinate of thickness direction, the origin locates in the end of the plate, θ (z) is the fiber angle of the location z, and a_k^A is defined as follows:

$$a_k^A = \frac{2k-N}{2N} \quad (2)$$

Coupling stiffness terms of asymmetrical laminates are represented with coupling lamination parameters. The coupling lamination parameters are defined as follows:

$$\boldsymbol{V}^{B}_{[1,2,3.4]^T} = \frac{4}{h^2}\int_{-\frac{h}{2}}^{\frac{h}{2}} z \begin{bmatrix} \cos 2\theta(z) \\ \cos 4\theta(z) \\ \sin 2\theta(z) \\ \sin 4\theta(z) \end{bmatrix} dz = \sum_{k=1}^{N} \left(a_k^B - a_{k-1}^B\right) \begin{bmatrix} \cos 2\theta_k \\ \cos 4\theta_k \\ \sin 2\theta_k \\ \sin 4\theta_k \end{bmatrix} \quad (3)$$

where

$$a_k^B = 2\left(\frac{2k-N}{2N}\right)^2 \quad (4)$$

Out-of-plane stiffness terms of asymmetrical laminates are represented with out-of-plane lamination parameters. The out-of-plane lamination parameters are defined as follows:

$$\boldsymbol{V}^{D}_{[1,2,3.4]^T} = \frac{12}{h^3}\int_{-\frac{h}{2}}^{\frac{h}{2}} z^2 \begin{bmatrix} \cos 2\theta(z) \\ \cos 4\theta(z) \\ \sin 2\theta(z) \\ \sin 4\theta(z) \end{bmatrix} dz = \sum_{k=1}^{N} \left(a_k^D - a_{k-1}^D\right) \begin{bmatrix} \cos 2\theta_k \\ \cos 4\theta_k \\ \sin 2\theta_k \\ \sin 4\theta_k \end{bmatrix} \quad (5)$$

where

$$a_k^D = 4\left(\frac{2k-N}{2N}\right)^3 \quad (6)$$

For most of practical laminated composite structures, fiber angle is limited to small set such as 0º, 45º, –45º, and 90º because of lack of experimental data and fabrication process. Let us consider the case that the fiber angle is limited to the small set. The values of $\sin 4\theta_k$ in Eqs. (1), (3) and (5), therefore, are always equal to zero, all values of $\boldsymbol{V}^{A,\ B,\ D}_{\ 4}$ are equal to zero. This makes the reduced lamination parameter vectors of three dimensions.

2.2 Response Surface Method

An objective function is approximated using response surface methodology [19]. The method provides approximation function between predictor variables and a response. In this study, the response f

is approximated with response surface of a quadratic polynomial.

$$y = \beta_0 + \sum_{i=1}^{M} \beta_i x_i + \sum_{i=1, j\geq i}^{M} \beta_{ij} x_i x_j \tag{7}$$

where β is the unknown coefficient, x is predictor variables, and M is the number of predictor variables. The unknown coefficient are estimated with a least-square-error method of a linear multiple regression.

To judge the performance of the approximation of the response surface, the adjusted coefficient of multiple determination R_{adj}^2 (R-square-adjusted) is used:

$$R_{adj}^2 = 1 - \frac{SS_E/(n-k-1)}{S_{yy}/(n-1)} \tag{8}$$

where S_{yy} is the total sum of squares, SS_E is square sum of errors, n is the number of experiments, and the k is the total number of unknown coefficients. Each coefficient of the response surface can be tested by using t-statistic.

In the present study, the variables are in-plane, out-of-plane, and coupling lamination parameters, $\boldsymbol{V}^A_{1,2,3}$, $\boldsymbol{V}^D_{1,2,3}$, and $\boldsymbol{V}^B_{1,2,3}$, and the response y is the objective function. We adopt quadratic polynomials for the function of response surface [20]. For the simplicity, when substituting as $\boldsymbol{V}^A_{1,2,3} = \boldsymbol{V}^A$, $\boldsymbol{V}^B_{1,2,3} = \boldsymbol{V}^B$, and $\boldsymbol{V}^D_{1,2,3} = \boldsymbol{V}^D$ the response surface is expressed as follows:

$$f\left(\mathbf{V}^A, \mathbf{V}^B, \mathbf{V}^D\right) = c + \begin{bmatrix} \mathbf{V}^{A^T} & \mathbf{V}^{B^T} & \mathbf{V}^{D^T} \end{bmatrix} \begin{bmatrix} \mathbf{b}_{V^A} \\ \mathbf{b}_{V^B} \\ \mathbf{b}_{V^D} \end{bmatrix} + \frac{1}{2} \begin{bmatrix} \mathbf{V}^{A^T} & \mathbf{V}^{B^T} & \mathbf{V}^{D^T} \end{bmatrix} \begin{bmatrix} \mathbf{A}_{V^A V^A} & \mathbf{A}_{V^A V^B} & \mathbf{A}_{V^A V^D} \\ \mathbf{A}^T_{V^A V^B} & \mathbf{A}_{V^B V^B} & \mathbf{A}_{V^B V^D} \\ \mathbf{A}^T_{V^A V^D} & \mathbf{A}^T_{V^B V^D} & \mathbf{A}_{V^D V^D} \end{bmatrix} \begin{bmatrix} \mathbf{V}^A \\ \mathbf{V}^B \\ \mathbf{V}^D \end{bmatrix} \tag{9}$$

where c, $\boldsymbol{b}$, $\boldsymbol{A}$ is the unknown constant, vector, and matrix coefficients. Because the number of unknown coefficients of the response surface of the quadratic polynomials is 55, 110 laminates are needed for the accurate approximation empirically. To select best set of 110 stacking sequences from all feasible stacking sequence, D-optimal design of experiments (DOE) methods is used. The minimum variance of the coefficient can be obtained by using the DOE.

2.3 Fractal Pattern of Feasible Laminates

When the fiber angle is limited to a small set such as 0º, 45º, –45º and 90º, all values of the in-plane, out-of-plane, coupling lamination parameters defined in Eqs. (1), (3) and (5) are expressed as follows:

$$\boldsymbol{V}^X_{[1,2,3]^T} = s^X_0 \boldsymbol{n}_0 + s^X_{45} \boldsymbol{n}_{45} + s^X_{90} \boldsymbol{n}_{90} + s^X_{-45} \boldsymbol{n}_{-45} \tag{10}$$

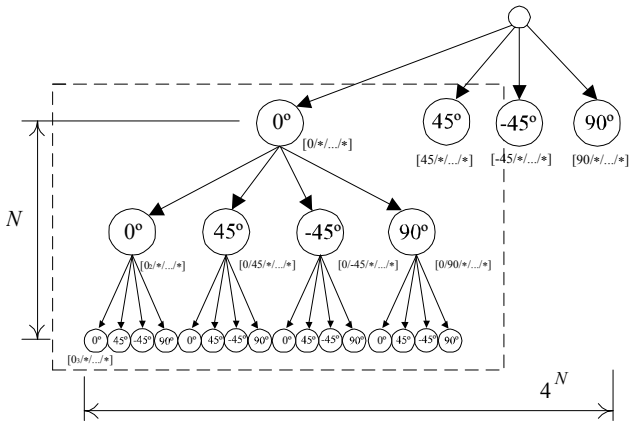

Fig. 1. Fractal branch structure of a stacking sequence tree.

with X=A, B, D

where $\boldsymbol{n}$ is the vectors of each fiber angle and s is the coefficient defined as follows:

$$\boldsymbol{n}_0 = \begin{bmatrix} 1 \\ 1 \\ 0 \end{bmatrix}, \boldsymbol{n}_{45} = \begin{bmatrix} 0 \\ -1 \\ 1 \end{bmatrix}, \boldsymbol{n}_{90} = \begin{bmatrix} -1 \\ 1 \\ 0 \end{bmatrix}, \boldsymbol{n}_{-45} = \begin{bmatrix} 0 \\ -1 \\ -1 \end{bmatrix} \tag{11}$$

$$s^X_j = \sum_{k=1}^{N} \delta_k \left(a^X_k - a^X_{k-1}\right) \tag{12}$$

δ_k= 1 when $\theta_k = \theta_j$ with j = 0º, ±45º, 90º

δ_k= 0 when $\theta_k \neq \theta_j$ with j = 0º, ±45º, 90º

The coefficient s in Eq. (10) satisfies the following equations per Eqs. (1), (3), and (5):

$$0 \leq s^X_j \leq 1 \quad \text{with } X = A, D \tag{13}$$

$$-1/2 \leq s^B_j \leq 1/2 \tag{14}$$

$$s^X_0 + s^X_{45} + s^X_{-45} + s^X_{90} = 1 \quad \text{with } X = A, D \tag{15}$$

$$s^B_0 + s^B_{45} + s^B_{-45} + s^B_{90} = 0 \tag{16}$$

The Eqs. (13) and (15) indicate that any vector of in-plan and out-of-plane lamination parameters, $\boldsymbol{V}^A_{1,2,3}$ and $\boldsymbol{V}^D_{1,2,3}$, can be plotted inside of the tetrahedron represented by four vectors defined in Eq. (11): (1, 1, 0), (0, –1, 1), (–1, 1, 0), and (0, –1, –1).

In the proposed fractal branch-and-bound method for asymmetrical laminates, the optimal stacking sequence is searched from outer layers of both sides because the outer layers have more effect on the out-of-plane and coupling lamination parameters indicated in Eqs. (3) and (5) [21]. An entire set of the feasible stacking sequence can be expressed as a large tree as shown in Fig. 1. Let us consider the following general case that outer d plies in N total plies have been already decided:

$[\theta_1/\theta_3/\ldots/\theta_{d-1}/*/\ldots/*/\theta_d/\ldots/\theta_4/\theta_2]$ when d is even (17)

$[\theta_1/\theta_3/\ldots/\theta_d/*/\ldots/*/\theta_{d-1}/\ldots/\theta_4/\theta_2]$ when d is odd (18)

where θ is the decided fiber angle and asterisk means the undecided fiber angle.

The in-plane and out-of-plane lamination parameters, $\boldsymbol{V}^A{}_{1,\,2,\,3}$ and $\boldsymbol{V}^D{}_{1,\,2,\,3}$, in case of the stacking sequence in Eqs. (17) and (18) are as follows:

$$\boldsymbol{V}^X_{[1,2,3]^T} = \boldsymbol{V}^X_0 + s^X_0\boldsymbol{n}_0 + s^X_{45}\boldsymbol{n}_{45} + s^X_{90}\boldsymbol{n}_{90} + s^X_{-45}\boldsymbol{n}_{-45} \quad \text{with } X=A,\,D \qquad (19)$$

where $\boldsymbol{V}^X{}_0$ and $s_j{}^X$ are defined as follows:

$$\boldsymbol{V}^X_0 = \sum_{k=1}^{d/2}\left(a^X_k - a^X_{k-1}\right)\begin{bmatrix}\cos 2\theta_k\\ \cos 4\theta_k\\ \sin 2\theta_k\end{bmatrix} + \sum_{k=N-d/2+1}^{N}\left(a^X_k - a^X_{k-1}\right)\begin{bmatrix}\cos 2\theta_k\\ \cos 4\theta_k\\ \sin 2\theta_k\end{bmatrix} \quad \text{when } d \text{ is even} \qquad (20)$$

$$\boldsymbol{V}^X_0 = \sum_{k=1}^{(d+1)/2}\left(a^X_k - a^X_{k-1}\right)\begin{bmatrix}\cos 2\theta_k\\ \cos 4\theta_k\\ \sin 2\theta_k\end{bmatrix} + \sum_{k=N-(d-3)/2}^{N}\left(a^X_k - a^X_{k-1}\right)\begin{bmatrix}\cos 2\theta_k\\ \cos 4\theta_k\\ \sin 2\theta_k\end{bmatrix} \quad \text{when } d \text{ is odd} \qquad (21)$$

$$s^X_j = \sum_{k=d/2+1}^{N-d/2}\delta\left(a^X_k - a^X_{k-1}\right) \quad \text{when } d \text{ is even} \qquad (22)$$

$$s^X_j = \sum_{k=(d+1)/2+1}^{N-(d-1)/2}\delta\left(a^X_k - a^X_{k-1}\right) \quad \text{when } d \text{ is odd} \qquad (23)$$

The sum of coefficients s_j in Eqs. (22) and (23) are equal to $(a^X{}_{N-d/2} - a^X{}_{d/2})$ and $(a^X{}_{N-(d-1)/2} - a^X{}_{(d+1)/2})$, respectively. Let us rewrite the coefficient s as follows:

$$p^X_j = \frac{1}{a^X_{N-d/2} - a^X_{d/2}}s^X_j \quad \text{when } d \text{ is even} \qquad (24)$$

$$p^X_j = \frac{1}{a^X_{N-(d-1)/2} - a^X_{(d+1)/2}}s^X_j \quad \text{when } d \text{ is odd} \qquad (25)$$

This expression indicates that coefficient p satisfies the Eqs. (13) and (15) and that the coefficients are treated as the same as the coefficient s. Using this p, the in-plane and out-of-plane lamination parameters, $\boldsymbol{V}^A$ and $\boldsymbol{V}^D$, of the laminates in Eqs. (17) and (18) are rewritten as follows:

$$\boldsymbol{V}^X = \boldsymbol{V}^X_0 + \left(a^X_{N-d/2} - a^X_{d/2}\right)\boldsymbol{V}^X_d \quad \text{when } d \text{ is even} \qquad (26)$$

$$\boldsymbol{V}^X = \boldsymbol{V}^X_0 + \left(a^X_{N-(d-1)/2} - a^X_{(d+1)/2}\right)\boldsymbol{V}^X_d \quad \text{when } d \text{ is odd} \qquad (27)$$

with $X = A,\,D$

where $\boldsymbol{V}^X{}_0$ and $\boldsymbol{V}^X{}_d$ are defined as follows:

$$\boldsymbol{V}^X_0 = \sum_{k=1}^{d/2}\left(a^X_k - a^X_{k-1}\right)\begin{bmatrix}\cos 2\theta_k\\ \cos 4\theta_k\\ \sin 2\theta_k\end{bmatrix} + \sum_{k=N-d/2+1}^{N}\left(a^X_k - a^X_{k-1}\right)\begin{bmatrix}\cos 2\theta_k\\ \cos 4\theta_k\\ \sin 2\theta_k\end{bmatrix} \quad \text{when } d \text{ is even} \qquad (28)$$

$$\boldsymbol{V}^X_0 = \sum_{k=1}^{(d+1)/2}\left(a^X_k - a^X_{k-1}\right)\begin{bmatrix}\cos 2\theta_k\\ \cos 4\theta_k\\ \sin 2\theta_k\end{bmatrix} + \sum_{k=N-(d-3)/2}^{N}\left(a^X_k - a^X_{k-1}\right)\begin{bmatrix}\cos 2\theta_k\\ \cos 4\theta_k\\ \sin 2\theta_k\end{bmatrix} \quad \text{when } d \text{ is odd} \qquad (29)$$

$$\boldsymbol{V}^X_d = p^X_0\boldsymbol{n}_0 + p^X_{45}\boldsymbol{n}_{45} + p^X_{90}\boldsymbol{n}_{90} + p^X_{-45}\boldsymbol{n}_{-45} \qquad (30)$$

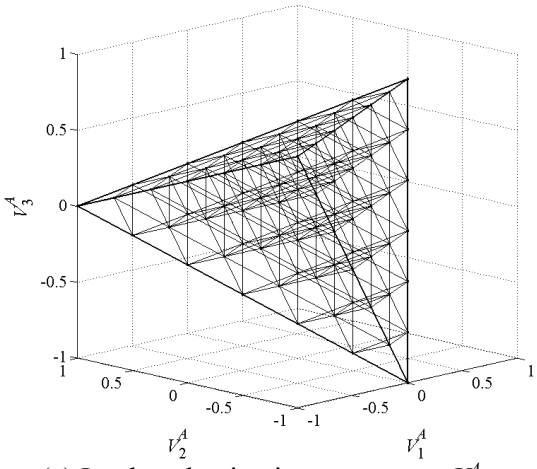

(a) In-plane lamination parameter, $V^A{}_{1,\,2,\,3}$.

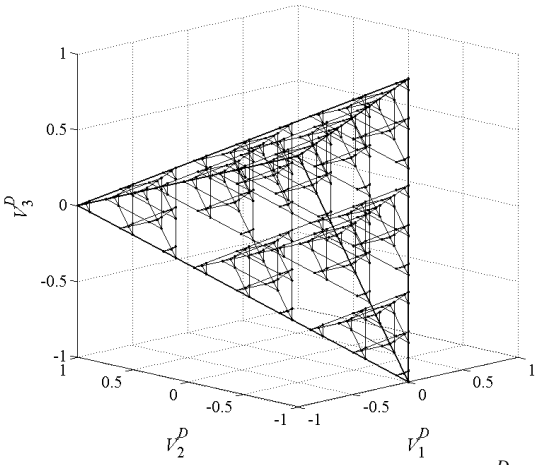

(b) Out-of-plane lamination parameter, $V^D{}_{1,\,2,\,3}$.

Fig. 2. Fractal tetrahedron pattern of feasible laminates drawn by plotting all feasible laminates of six plies in lamination parameters.

Eqs. (26) and (27) indicate that the laminates expressed by Eqs. (17) and (18) create self-similar tetrahedrons of which the center points are moved to $\boldsymbol{V}^A{}_0$ and $\boldsymbol{V}^D{}_0$, respectively. These are self-similar shrunk tetrahedrons by the factor $(r^{A,D}{}_d)$ of $(a^{A,D}{}_{N-d/2} - a^{A,D}{}_{d/2})$ and $(a^{A,D}{}_{N-(d-1)/2} - a^{A,D}{}_{(d+1)/2})$. Similarly, the self-similar smaller tetrahedrons are created inside of the tetrahedron as the fiber angle is decided from outer-ply. This process creates a fractal pattern of all feasible laminates. When the total plies of laminates N are six, fractal pattern of all self-similar tetrahedrons is shown in Fig. 2.

On the contrary, the coefficient s of coupling lamination parameters is expressed as Eqs. (14) and (16), and does not satisfy Eqs. (13) and (15). This indicates that the coupling lamination parameters are not always plotted inside the tetrahedron represented by the four vectors defined in Eq. (11), which means

the coupling lamination parameters $\boldsymbol{V}^B_{1,2,3}$ does not create a tetrahedral fractal pattern.

To clarify the feasible region of the coupling lamination parameters $\boldsymbol{V}^B_{1,2,3}$, Eq. (3) in case that total number of laminates N are even number is rewritten as follows:

$$\boldsymbol{V}^B_{[1,2,3]^T} = \sum_i \sum_j s^B_{i/j} \boldsymbol{n}_{i/j} \quad \text{with} \quad i,j = 0, \pm 45, 90 \tag{31}$$

where the coefficient s and vectors $\boldsymbol{n}$ are defined as follows:

$$s^B_{i/j} = 2 \sum_{k=N/2+1}^{N} \delta_k \left(a^B_k - a^B_{k-1} \right) \tag{32}$$

$\delta_k = 1$ when $\theta_k = \theta_i$ and $\theta_{N-k+1} = \theta_i$

$\delta_k = 0$ when $\theta_k \neq \theta_j$ or $\theta_{N-k+1} \neq \theta_i$

$$\boldsymbol{n}_{i/j} = \frac{-\boldsymbol{n}_i + \boldsymbol{n}_j}{2} \tag{33}$$

Even if the N is odd number, the procedures are similar to in case of even number except for treatment of the mid layer ($\boldsymbol{V}^B_{1,2,3}=0$).

From $\boldsymbol{n}_{i/i} = 0$, Eq. (31) is rewritten as follows:

$$\begin{aligned}\boldsymbol{V}^B_{[1,2,3]^T} = {} & s^B_{0/45}\boldsymbol{n}_{0/45} + s^B_{0/90}\boldsymbol{n}_{0/90} + s^B_{0/-45}\boldsymbol{n}_{0/-45} + s^B_{45/0}\boldsymbol{n}_{45/0} + \\ & s^B_{45/90}\boldsymbol{n}_{45/90} + s^B_{45/-45}\boldsymbol{n}_{45/-45} + s^B_{90/0}\boldsymbol{n}_{90/0} + s^B_{90/45}\boldsymbol{n}_{90/45} + \\ & s^B_{90/-45}\boldsymbol{n}_{90/-45} + s^B_{-45/0}\boldsymbol{n}_{-45/0} + s^B_{-45/45}\boldsymbol{n}_{-45/45} + s^B_{-45/90}\boldsymbol{n}_{-45/90}\end{aligned} \tag{34}$$

where

$$\boldsymbol{n}_{0/45} = \begin{bmatrix} -1/2 \\ -1 \\ 1/2 \end{bmatrix}, \boldsymbol{n}_{0/90} = \begin{bmatrix} -1 \\ 0 \\ 0 \end{bmatrix}, \boldsymbol{n}_{0/-45} = \begin{bmatrix} -1/2 \\ -1 \\ -1/2 \end{bmatrix},$$

$$\boldsymbol{n}_{45/0} = \begin{bmatrix} 1/2 \\ -1 \\ -1/2 \end{bmatrix}, \boldsymbol{n}_{45/90} = \begin{bmatrix} -1/2 \\ 1 \\ -1/2 \end{bmatrix}, \boldsymbol{n}_{45/-45} = \begin{bmatrix} 0 \\ 0 \\ -1 \end{bmatrix}, \tag{35}$$

$$\boldsymbol{n}_{90/0} = \begin{bmatrix} 1 \\ 0 \\ 0 \end{bmatrix}, \boldsymbol{n}_{90/45} = \begin{bmatrix} 1/2 \\ -1 \\ 1/2 \end{bmatrix}, \boldsymbol{n}_{90/-45} = \begin{bmatrix} 1/2 \\ -1 \\ -1/2 \end{bmatrix},$$

$$\boldsymbol{n}_{-45/0} = \begin{bmatrix} 1/2 \\ 1 \\ 1/2 \end{bmatrix}, \boldsymbol{n}_{-45/45} = \begin{bmatrix} 0 \\ 0 \\ 1 \end{bmatrix}, \boldsymbol{n}_{-45/90} = \begin{bmatrix} -1/2 \\ 1 \\ 1/2 \end{bmatrix}$$

The coefficient s in Eq. (34) satisfies the following equation per the definition of s in Eq. (32).

$$0 \le s^B_{i/j} \le 1 \tag{36}$$

$$\begin{aligned}& s^B_{0/45} + s^B_{0/90} + s^B_{0/-45} + s^B_{45/0} + s^B_{45/90} + s^B_{45/-45} + \\ & s^B_{90/0} + s^B_{90/45} + s^B_{90/-45} + s^B_{-45/0} + s^B_{-45/45} + s^B_{-45/90} \\ & = 1 - s^B_{0/0} - s^B_{45/45} - s^B_{90/90} - s^B_{-45/-45} \le 1\end{aligned} \tag{37}$$

Eqs. (36) and (37) indicate that any vector of coupling lamination parameters $\boldsymbol{V}^B_{1,2,3}$ can be plotted inside of the tetradecahedron represented by 12 vectors defined in Eq. (35) as shown in Fig. 3 [22].

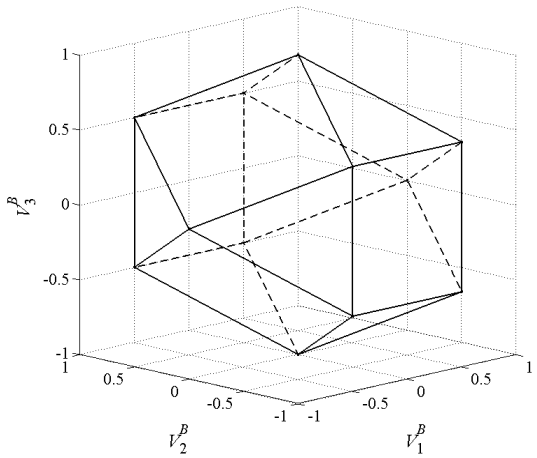

Fig. 3. Feasible region of coupling lamination parameter, $\boldsymbol{V}^B_{1,2,3}$.

As is the case with in-plan and out-of-plane lamination parameters, let us consider the general case that outer d plies in N total plies have been already decided as shown in Eq. (17). The coupling lamination parameters $\boldsymbol{V}^B_{1,2,3}$ of the laminates are expressed as follows:

$$\boldsymbol{V}^B_{[1,2,3]^T} = \boldsymbol{V}^B_0 + \sum_i \sum_j s^B_{i/j} \boldsymbol{n}_{i/j} \quad \text{with} \quad i,j = 0, \pm 45, 90 \tag{38}$$

where $\boldsymbol{V}^B_0$ and $s^B_{i/j}$ are defined as follows:

$$\boldsymbol{V}^B_0 = \sum_{k=1}^{d/2} \left(a^B_k - a^B_{k-1} \right) \begin{bmatrix} \cos 2\theta_k \\ \cos 4\theta_k \\ \sin 2\theta_k \end{bmatrix} + \sum_{k=N-d/2+1}^{N} \left(a^B_k - a^B_{k-1} \right) \begin{bmatrix} \cos 2\theta_k \\ \cos 4\theta_k \\ \sin 2\theta_k \end{bmatrix} \tag{39}$$

$$s^B_{i/j} = 2 \sum_{k=N/2+1}^{N-d/2} \delta_k \left(a^B_k - a^B_{k-1} \right) \tag{40}$$

The sum of coefficient s in Eq. (40) is equal to $2a^B_{N-d/2}$. And let us rewrite the coefficient s as follows:

$$p^B_{i/j} = \frac{1}{2a^B_{N-d/2}} s^B_{i/j} \tag{41}$$

Eq. (41) indicates that coefficient p satisfies the Eqs. (36) and (37) and are treated as s. Using this p, the coupling lamination parameters $\boldsymbol{V}^B$ of the laminates shown in Eq. (17) are expressed as follows:

$$\boldsymbol{V}^B = \boldsymbol{V}^B_0 + 2a^B_{N-d/2} \boldsymbol{V}^B_d \tag{42}$$

where

$$\begin{aligned}\boldsymbol{V}^B_d = {} & p^B_{0/45}\boldsymbol{n}_{0/45} + p^B_{0/90}\boldsymbol{n}_{0/90} + p^B_{0/-45}\boldsymbol{n}_{0/-45} + \\ & p^B_{45/0}\boldsymbol{n}_{45/0} + p^B_{45/90}\boldsymbol{n}_{45/90} + p^B_{45/-45}\boldsymbol{n}_{45/-45} + p^B_{90/0}\boldsymbol{n}_{90/0} + \\ & p^B_{90/45}\boldsymbol{n}_{90/45} + p^B_{90/-45}\boldsymbol{n}_{90/-45} + p^B_{-45/0}\boldsymbol{n}_{-45/0} + p^B_{-45/45}\boldsymbol{n}_{-45/45} + \\ & p^B_{-45/90}\boldsymbol{n}_{-45/90}\end{aligned} \tag{43}$$

Eqs. (42) and (43) indicate that the laminates in Eq. (17) create self-similar tetradecahedrons of

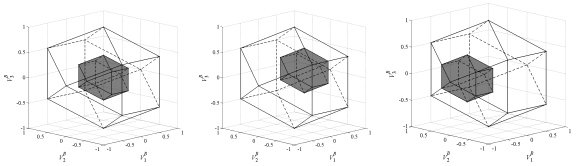

(a) [θ_1/∗/…/∗/ θ_1] (b) [0/∗/…/∗/45] (c) [0/∗/…/∗/90]

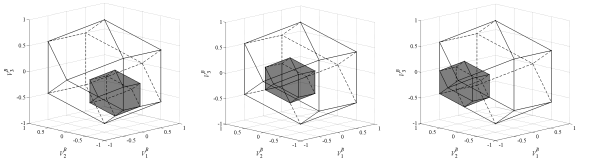

(d) [0/∗/…/∗/–45] (e) [45/∗/…/∗/0] (f) [45/∗/…/∗/90]

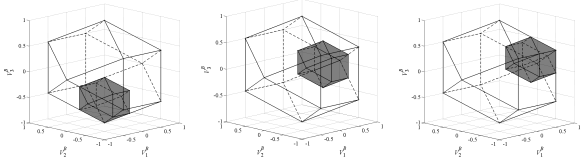

(g) [45/∗/…/∗/–45] (h) [90/∗/…/∗/0] (i) [90/∗/…/∗/45]

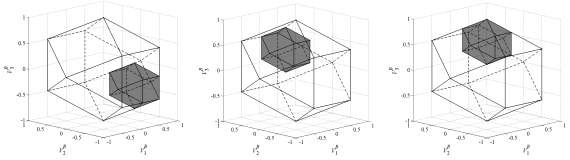

(j) [90/∗/…/∗/–45] (k) [–45/∗/…/∗/0] (l) [–45/∗/…/∗/45]

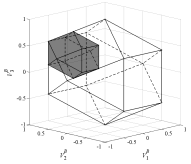

(m) [–45/∗/…/∗/90]

Fig. 4. Feasible regions of coupling lamination parameter when [θ_1/∗/…/∗/ θ_2] of six plies.

which the center points are moved to $\boldsymbol{V}_0^B$. This is a self-similar shrunk tetradecahedron by the factor r_d^B of $2a^B_{N\text{-}d\ /\ 2}$. Similarly, the self-similar smaller tetrahedrons are created inside of the tetrahedron as the fiber angle is decided from outer-ply. This process creates a fractal pattern of all feasible laminates. When the fiber angles of two outer layers in the total six plies are decided, [θ_1/∗/.../∗/θ_2], the shrunk self-similar tetradecahedrons are shown in Fig. 4 (a)-(m). Fig. 5 shows the more shrunk tetradecahedrons when the two outer fiber angle is decided: [0/θ_1/∗/.../∗/θ_2/90].

In case that the odd d layers are decided as shown in Eq. (18), the feasible region of coupling lamination parameters are created inside of the irregular tetradecahedron including four tetradecahedrons when even (d+1) layers is decided. For example, let us consider the laminates [0/∗/…/∗] (d=1, θ_1=0º, N=6). The feasible region of coupling

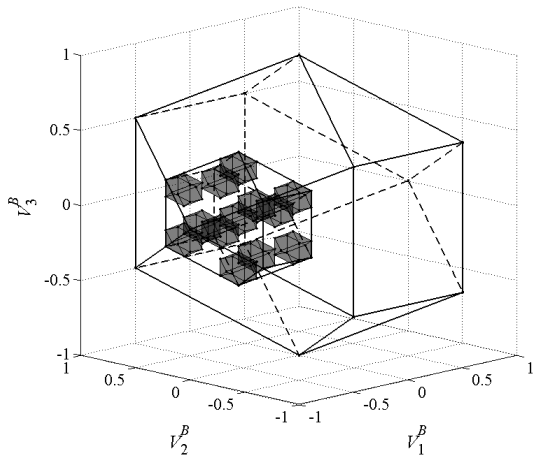

Fig. 5. Feasible regions of coupling lamination parameter when [0/θ_1/∗/∗/θ_2/ 90] of six plies (θ_1, θ_2=0, ±45, 90).

lamination parameters of the laminates includes four tetradecahedrons of [0/∗/…/∗/0], [0/∗/…/∗/45], [0/∗/…/∗/90], [0/∗/…/∗/-45] as shown in Fig. 4(a)-(d), and creates the irregular tetradecahedron. Fig. 6 shows all tetradecahedrons in case of the laminates of N=6. As you can see, the tetradecahedrons creates a fractal pattern.

Fig. 7 shows the shrunk factor of self-similar tetrahedrons and tetradecahedrons to original tetrahedrons and tetradecahedrons of in-plane, out-of-plane or coupling lamination parameters. In Fig. 7, the abscissa is the number of decided layers d, and the ordinate is the shrunk factor, r_d^A, r_d^B and r_d^D of in-plane, coupling and out-of-plane lamination parameters. The open triangle symbol indicates r_d^B when the fiber angle is decided from outer layers of both sides as Eqs. (17) and (18), and the solid triangle symbol indicates r_d^B when the fiber angle is decided from the outer layers from one side as follows:

$$[\theta_1/\theta_2/\ldots/\theta_d/*/\ldots/*] \tag{44}$$

As shown in Fig. 7, the shrunk factor of both sides is smaller than that of one side. This means that deciding the fiber angles from outer layers of both sides limits the feasible region of laminate parameters strictly at an early stage in process of deciding the fiber angles, which decreases the computational cost.

2.4 Fractal Branch and Bound Method

The feasible regions of in-plane, out-of-plane and coupling lamination parameters of undecided laminates $\boldsymbol{V}^A_{1,\,2,\,3}$, $\boldsymbol{V}^D_{1,\,2,\,3}$ and $\boldsymbol{V}^B_{1,\,2,\,3}$ is converged

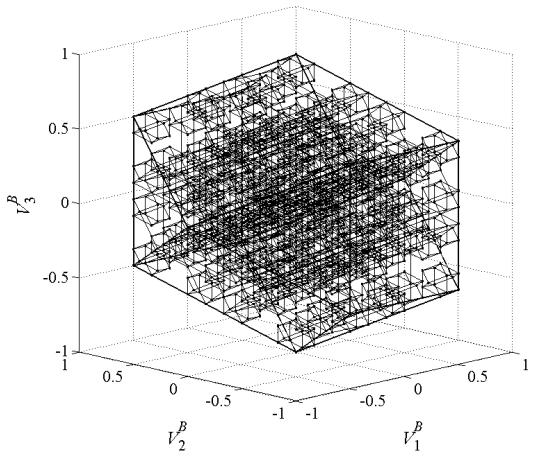

Fig. 6. Fractal tetradecahedron pattern of feasible laminates drawn by plotting all feasible laminates of six plies in coupling lamination parameters.

into the smaller self-similar tetrahedrons or tetradecahedrons inside of the original tetrahedrons or tetradecahedrons as the fiber angles are decided from outer layers.

In the fractal branch-and-bound method, a branch-and-bound method is performed to obtain the optimal stacking-sequence, which maximizes the response surface of an objective function. For the branch-and-bound method, an efficient evaluation function prunes inefficient branches during searching. Evaluating the objective function at each branch can be performed using response surface function. To evaluate the fractal branch safely, Eq. (26), (27) and (42) is substituted into Eq. (9). The objective function is transformed as follows:

$$\begin{aligned} f &= f\left(\boldsymbol{V}^A, \boldsymbol{V}^B, \boldsymbol{V}^D\right) \\ &= f\left(\boldsymbol{V}_0^A + r_d^A \boldsymbol{V}_d^A, \boldsymbol{V}_0^B + r_d^B \boldsymbol{V}_d^B, \boldsymbol{V}_0^D + r_d^D \boldsymbol{V}_d^D\right) \\ &= f_0 + f'_{\boldsymbol{V}^A} + f'_{\boldsymbol{V}^B} + f'_{\boldsymbol{V}^D} + f'_{\boldsymbol{V}^A\boldsymbol{V}^B} + f'_{\boldsymbol{V}^B\boldsymbol{V}^D} + f'_{\boldsymbol{V}^D\boldsymbol{V}^A} \end{aligned} \tag{45}$$

where

$$\begin{aligned} f_0 &= f\left(\boldsymbol{V}_0^A, \boldsymbol{V}_0^B, \boldsymbol{V}_0^D\right) \\ f'_{\boldsymbol{V}^A} &= r_d^A \boldsymbol{V}_d^{AT} \boldsymbol{b}'_{\boldsymbol{V}^A} + \left(r_d^A\right)^2 \frac{1}{2} \boldsymbol{V}_d^{AT} \left[\boldsymbol{A}_{\boldsymbol{V}^A\boldsymbol{V}^A}\right] \boldsymbol{V}_d^A \\ f'_{\boldsymbol{V}^B} &= r_d^B \boldsymbol{V}_d^{BT} \boldsymbol{b}'_{\boldsymbol{V}^B} + \left(r_d^B\right)^2 \frac{1}{2} \boldsymbol{V}_d^{BT} \left[\boldsymbol{A}_{\boldsymbol{V}^B\boldsymbol{V}^B}\right] \boldsymbol{V}_d^B \\ f'_{\boldsymbol{V}^D} &= r_d^D \boldsymbol{V}_d^{DT} \boldsymbol{b}'_{\boldsymbol{V}^D} + \left(r_d^D\right)^2 \frac{1}{2} \boldsymbol{V}_d^{DT} \left[\boldsymbol{A}_{\boldsymbol{V}^D\boldsymbol{V}^D}\right] \boldsymbol{V}_d^D \\ f'_{\boldsymbol{V}^A\boldsymbol{V}^B} &= r_d^A r_d^B \boldsymbol{V}_0^A \left[\boldsymbol{A}_{\boldsymbol{V}^A\boldsymbol{V}^B}\right] \boldsymbol{V}_0^B \\ f'_{\boldsymbol{V}^B\boldsymbol{V}^D} &= r_d^B r_d^D \boldsymbol{V}_0^B \left[\boldsymbol{A}_{\boldsymbol{V}^B\boldsymbol{V}^D}\right] \boldsymbol{V}_0^D \\ f'_{\boldsymbol{V}^D\boldsymbol{V}^A} &= r_d^D r_d^A \boldsymbol{V}_0^D \left[\boldsymbol{A}_{\boldsymbol{V}^D\boldsymbol{V}^A}\right] \boldsymbol{V}_0^A \end{aligned} \tag{46}$$

$$\begin{bmatrix} \boldsymbol{b}'_{\boldsymbol{V}^A} \\ \boldsymbol{b}'_{\boldsymbol{V}^B} \\ \boldsymbol{b}'_{\boldsymbol{V}^D} \end{bmatrix} = \begin{bmatrix} \boldsymbol{b}_{\boldsymbol{V}^A} \\ \boldsymbol{b}_{\boldsymbol{V}^B} \\ \boldsymbol{b}_{\boldsymbol{V}^D} \end{bmatrix} + \begin{bmatrix} \boldsymbol{A}_{\boldsymbol{V}^A\boldsymbol{V}^A} & \boldsymbol{A}_{\boldsymbol{V}^A\boldsymbol{V}^B} & \boldsymbol{A}_{\boldsymbol{V}^A\boldsymbol{V}^D} \\ \boldsymbol{A}^T_{\boldsymbol{V}^A\boldsymbol{V}^B} & \boldsymbol{A}_{\boldsymbol{V}^B\boldsymbol{V}^B} & \boldsymbol{A}_{\boldsymbol{V}^B\boldsymbol{V}^D} \\ \boldsymbol{A}^T_{\boldsymbol{V}^A\boldsymbol{V}^D} & \boldsymbol{A}^T_{\boldsymbol{V}^B\boldsymbol{V}^D} & \boldsymbol{A}_{\boldsymbol{V}^D\boldsymbol{V}^D} \end{bmatrix} \begin{bmatrix} \boldsymbol{V}_0^A \\ \boldsymbol{V}_0^B \\ \boldsymbol{V}_0^D \end{bmatrix} \tag{47}$$

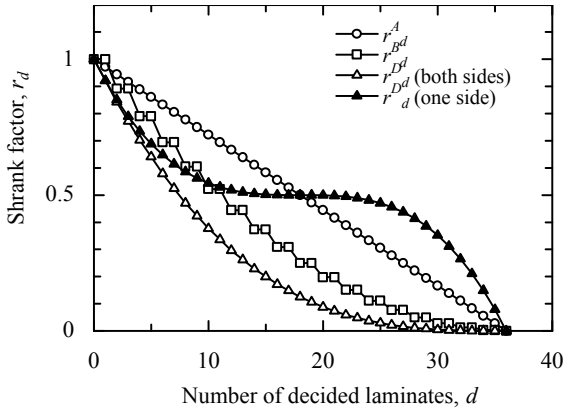

Fig. 7. Shrank factor of fractal pattern of 36 plies.

where f_0 is constant, $f'_{\boldsymbol{V}^A}$, $f'_{\boldsymbol{V}^B}$ and $f'_{\boldsymbol{V}^D}$ are quadratic polynomial of $\boldsymbol{V}^A$, $\boldsymbol{V}^B$ and $\boldsymbol{V}^D$, respectively. The $f'_{\boldsymbol{V}^A\boldsymbol{V}^B}$, $f'_{\boldsymbol{V}^B\boldsymbol{V}^D}$ and $f'_{\boldsymbol{V}^D\boldsymbol{V}^A}$ are the interaction terms of $\boldsymbol{V}^A$ and $\boldsymbol{V}^B$, $\boldsymbol{V}^B$ and $\boldsymbol{V}^D$, and $\boldsymbol{V}^D$ and $\boldsymbol{V}^A$, respectively.

The conservative estimation function g is defined as follows:

$$\begin{aligned} g = f_0 &+ \max f'_{\boldsymbol{V}^A} + \max f'_{\boldsymbol{V}^B} + \max f'_{\boldsymbol{V}^D} + \\ &\max f'_{\boldsymbol{V}^A\boldsymbol{V}^B} + \max f'_{\boldsymbol{V}^B\boldsymbol{V}^D} + \max f'_{\boldsymbol{V}^D\boldsymbol{V}^A} \end{aligned} \tag{48}$$

Since the estimation function g satisfies the following inequality, g is conservative estimation.

$$g \geq \max f \tag{49}$$

Each term of Eq. (48) corresponds to the maximum value in shrank tetrahedron or tetradecahedron. This each maximum value is obtained using quadratic polynomial function of response surface method as the objective function. The coupling lamination parameters $\boldsymbol{V}^B{}_{1,\,2,\,3}$ create the irregular tetradecahedrons when the number of the decided fiber angles is odd; it needs the redefinition of the feasible region repeatedly, and increases the computational cost. To reduce its consumption of high computational cost, the $\boldsymbol{V}^B$ region in case of odd d is substituted by the outer even $(d-1)$ tetradecahedrons.

Search of the optimal stacking-sequence starts from a provisional optimal laminates. The provisional optimal laminate is selected in a way that the fiber angle is decided from outer layers as maximizing the objective function at each branch with the once determined fiber angles fixed. Once the provisional optimal stacking sequence is selected, the fractal branch-and-bound method is used to obtain the optimal stacking sequence that maximizing the objective function. We start the searching of the branch of [0/*/.../*]. The shrunk tetrahedron and tetradecahedron of the branch of the

set of the laminates are easily calculated, and the maximum value of the response in the shrunk tetrahedron and tetradecahedron are also estimated. If the estimation value is lower than the provisional one, this means that any stacking sequence that has 0 deg ply at outermost layer does not have better objective value. The searching into the inner tetrahedral or tetradecahedron is aborted, which means the branch can be pruned. Otherwise, if estimated value is higher than the provisional one, it means the tetrahedron might have a better stacking sequence. The solution searching continues into the inner tetrahedrons or tetradecahedrons. This procedure is repeated until all branches are investigated and finally the optimum stacking sequence that maximizes the objective function is obtained.

In this study, to increase the accuracy of approximation, the modified response surface [23] is used as a response surface. In this modified response surface, the adjacent stacking-sequences around the optimal stacking-sequence obtained using fractal branch-and-bound method once is added into the experimental set of the response surface. And the fractal branch-and-bound method is performed using this modified response surface again. The adjacent stacking-sequences in in-plane and out-of-plane spaces are obtained, as is the similar case with symmetrical laminates [24]. The adjacent stacking-sequence of coupling lamination parameters is obtained by exchanging the each layer that exists on symmetrical geometry against mid-plane from Eqs. (1), (3) and (5). For example, when the stacking sequence is [90/45/45/0/0/45/0/45], the adjacent stacking sequence to be added is as follows:

(i) 1st layer ⇔ 8th layer:
[45/45/45/0/0/45/0/90]

(ii) 2nd layer ⇔ 7th layer:
[90/0/45/0/0/45/45/45]

(iii) 1st layer ⇔ 8th layer,
2nd layer ⇔ 7th layer:
[45/0/45/0/0/45/45/90]

These adjacent laminates have the same in-plan and out-of-plane lamination parameters and different coupling lamination parameters compared with those of the original laminates. The number of added stacking sequence, n_a, is as follows at most when the total number of plies is N.

$$n_a = \begin{cases} 2^{N/2} - 1 & \text{when } N \text{ is even} \\ 2^{(N-1)/2} - 1 & \text{when } N \text{ is odd} \end{cases} \quad (50)$$

3. Application of the proposed method

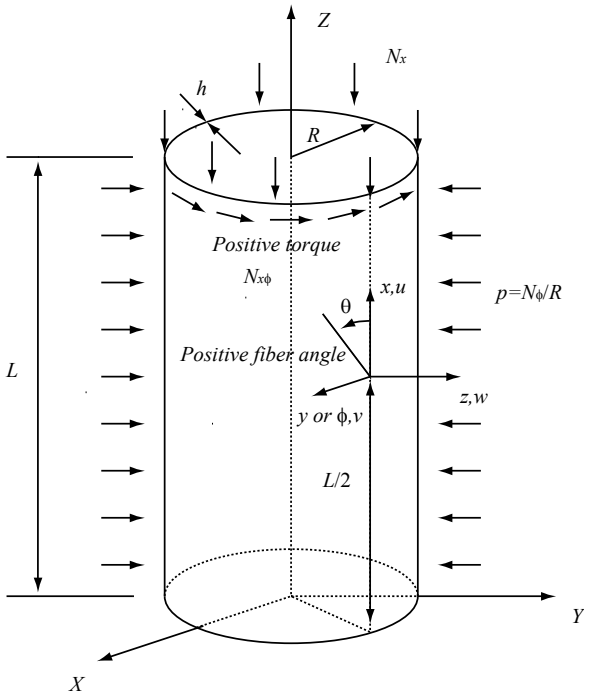

Fig. 8. Geometry of the laminated composite cylindrical shell.

3.1 Optimization Problem

The proposed improved fractal branch-and-bound method is applied to stacking sequence optimization of asymmetrical laminates for a buckling load maximization of cylindrical shells subjected to axial compression, external lateral pressure, and torsion [12, 22, 25]. The governing equation of composite cylindrical shell buckling based on Flügge's theory is expressed in terms of displacement at middle surface of the shells and in-plane stiffness matrix [***A***], coupling stiffness matrix [***B***], and out-of-plane stiffness [***D***] (See Ref. [25]). N_x, N_ϕ and $N_{x\phi}$ are the external axial compression per unit length, external lateral pressure ($p = N_\phi / R$), and torsional force per unit length.

The initial loads is expressed using loads N^0 as follows:

$$N_x^0 = q_x N^0, \; N_\phi^0 = q_\phi N^0, \; N_{x\phi}^0 = q_{x\phi} N^0 \quad (51)$$

where q_x, $q_{x\phi}$, and q_ϕ is the prescribed coefficient of axial compressive load, lateral pressure, and torsional load. When q_x, $q_{x\phi}$ and q_ϕ are given, a buckling load N_{cr} is obtained.

In the analysis, the material properties are used from a carbon/epoxy composite: E_{11}/E_{22} = 20, G_{12}/E_{22} = 0.6, ν_{12} = 0.25. The total number of laminates is 12, and the fiber angles are limited to 0º, ±45º, 90º. In the cylindrical shells, the L/R = 120,

Table 1. Optimization results.

Loading ratio				Laminate Config.	Parameter	Error
q_x	q_ϕ	$q_{x\phi}$			N	(%)
1	0	0	Fbbm	$[0_{12}]$	6.19	0.00
			Opt	$[0_{12}]$	6.19	–
0	1	0	Fbbm	$[90_5/0_2/90_5]$	12.49	-0.44
			Opt	$[90_{12}]$	12.54	–
0	0	1	Fbbm	$[90_3/0_4/-45_3/90_2]$	37.67	-2.28
			Opt	$[90_3/0_5/-45_2/90_2]$	38.55	–
1	0.5	0	Fbbm	$[90/0_{10}/90]$	6.98	0.00
			Opt	$[90/0_{10}/90]$	6.98	–
0.1	0	1	Fbbm	$[90_2/0_8/90_2]$	31.57	-1.63
			Opt	$[90_2/0_7/45/-45/90]$	32.09	–
0	0.05	1	Fbbm	$[90_3/0_4/-45_2/90_3]$	34.24	-0.52
			Opt	$[90_4/0_4/-45/90_3]$	34.42	–
0.1	0.05	1	Fbbm	$[90_3/0_6/-45/90_2]$	33.03	0.00
			Opt	$[90_3/0_6/-45/90_2]$	33.03	–

R/h = 20 as shown in Fig. 8. The objective function is the normalized buckling loads as follows [22]:

$$\overline{N} = N_{cr} / E_{22} h \times 10^3 \tag{52}$$

The normalized loads of axial compression, lateral pressure, and torsion are expressed as follows:

$$\overline{N}_x = q_x \overline{N},\ \overline{N}_\phi = q_\phi \overline{N},\ \overline{N}_{x\phi} = q_{x\phi} \overline{N} \tag{53}$$

3.2 Results and discussion

D-optimal DOE is used to select the 110 best laminates set from all 4^{12} = 16777216 laminates. Using this set of the laminates, the response surface of quadratic polynomial function is created in terms of in-plan, out-of-plane, and coupling lamination parameters, $V^{A,\,B,\,D}_{1,\,2,\,3}$. The adjusted coefficient of multiple determination R_{adj}^2 of the response surface is 0.972: which shows the approximation is enough accurate. Let us consider the condition that the cylinder is subjected to the torsional load: $q_x = q_\phi = 0$, and $q_{x\phi}$ = 1. Using the response surface and proposed fractal branch-and-bound method, the obtained optimal stacking-sequence is $[90_3/0_4/-45_3/90_2]$, and the buckling load parameter is 37.67. The true optimal stacking sequence obtained by searching around the lamination parameters of $[90_3/0_4/-45_3/90_2]$ is $[90_3/0_5/-45_2/90_2]$, and the buckling load parameter is 38.55. The relative error between the optimal value obtained using the fractal branch-and-bound method and the true value is 2.28 %. This value is small enough, and the obtained optimal laminate is practically acceptable.

Table 1 shows the stacking sequence optimization results with varying the ratio of axial compression, external lateral pressure and torsional force. In Table 1, q_x, q_ϕ and $q_{x\phi}$ show the ratio of external compressive load, external lateral pressure and torsional load, respectively. The relative error between optimal laminates obtained using proposed fractal branch-and-bound method and true optimal value is less than 2.28 %. This confirms that practical optimal stacking-sequence is obtained. The computational order is O (1.59^N) in the fractal branch-and-bound method and O (4^N) in Round Robin search as shown in Fig. 9.

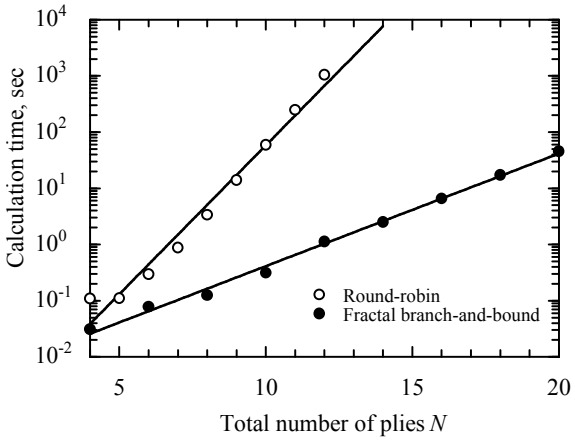

Fig. 9. CPU time of various total number of plies.

4. Concluding Remarks

For stacking-sequence optimization of asymmetrical laminates, we proposed the improved fractal branch-and-bound method. The stiffness of asymmetrical laminates is expressed in terms of in-plane, out-of-plane, and coupling lamination parameters. We clarify the feasible regions of the lamination parameters: the in-plane and out-of-plane lamination parameters create the fractal pattern of self-similar tetrahedrons, and the coupling lamination parameters create that of self-similar tetradecahedrons. The proposed method performs a branch-and-bound using the fractal pattern of lamination parameters, and effectively obtains an optimal stacking-sequence. To demonstrate the applicability of the method, we applied this method to the buckling-load maximization problems of cylinder shells subjected to axial compressive load, external lateral pressure and torsional load. As a result, the method is successfully applied, and the practical optimal stacking-sequence is obtained with low computational cost.

References

[1] Todoroki A., Haftka RT. "Stacking sequence optimization by a genetic algorithm with a new recessive gene like repair strategy". *Compos. B,* 29B, pp 277-285, 1998.
[2] Todoroki A., Ishikawa T. "Design of experiments for stacking sequence optimizations with genetic algorithm using response surface approximation". *Compos. Struct.*, 64, pp 349-357, 2004.
[3] Liu B., Haftka RT., Akgün MA., Todoroki A. "Permutation genetic algorithm for stakcing sequence design of composite laminates". *Comput. Methods Appl. Mech. Engrg.* 186, pp 357-372, 2000.
[4] Miki M. "Design of laminated fibrous composite plates with required flexural stiffness". *ASTM STP,* 864, pp 387-400, 1985.
[5] Fukunaga H., Chou TW. "Simplified design techniques for laminated cylindrical pressure vessels under stiffness and strength constraints". *J. Compos. Mater.*, 22, pp 1156-1169, 1998.
[6] Terada Y, Todoroki A, Shimamura Y. "Stacking sequence optimizations using fractal branch and bound method for laminated composites". *JSME Int. J. A*, 44(4), pp 490-498, 2001.
[7] Todoroki A, Terada Y. "Improved fractal branch and bound method for stacking-sequence optimizations of laminates". *AIAA J.*, 42(1), pp 141-148, 2004.
[8] Hirano Y., Todoroki A., "Stacking sequence optimizations for composite laminates using fractal branch and bound method (application for supersonic panel flutter problem with buckling load condition)". *Adv. Compos. Mater.*, 13(2), pp 89-107, 2004.
[9] Hirano Y., Todoroki A., "Stacking-sequence optimization of composite delta wing to improve flutter limit using fractal branch and bound method". *JSME Int. J. A*, 48(2), pp 65-72, 2005.
[10] Walker M, Reiss T, Adali S. "Multiobjective design of laminated cylindrical shells for maximum torsional and axial buckling loads". *Comput. Struct.*, 62(2), pp 237-242, 1997.
[11] Onoda J. "Optimal laminate configurations of cylindrical shells for axial buckling". *AIAA J.*, 23(7), pp 1093-1098, 1985.
[12] Diaconu CG., Sato M., Sekine H. "Buckling characteristics and layup optimization of long laminated composite cylindrical shells subjected to combined loads using lamination parameters". *Compos. Struct.*, 58, pp 423-433, 2002.
[13] Diaconu CG., Sato M., Sekine H. "Feasible region in general design space of lamination parameters for laminated composites". *AIAA J.*,40(3), pp 559-565, 2002.
[14] Zhou F., Ogawa A, Hashimoto R. "Deformation of antisymmetric laminate under centrifugal force and/or thermal load". *Compos. Struct.*, 51, pp 335-344, 2001.
[15] Buter A., Breitbach E. "Adaptive blade twist – calculations and experimental results". *Aerosp. Sci, Technol.* 4, pp 309-319, 2000.
[16] Sqminathan K., Ragounadin D. "Analytical solution using a higher-order refined theory for the static analysis of antisymmetric angle-ply composite and sandwich plates". *Compos. Struct.,* 64, pp 405-417, 2004.
[17] Loughlan J. "The influence of mechanical couplings on the compressive stability of anti-symmetrical angle-ply laminates". *Compos. Struct.*, 57, pp 473-482, 2002.
[18] Makeev A., Armanios E. "On a higher order analysis of laminates composite with extension-twist coupling". *Int. J. Solids Struct.*, 36, pp 1081-1098, 1999.
[19] Myers RH., Montgomery DC. "*Response surface methodology: process and product optimization using designed experiments*". New York: John Wiley & Sons, Inc; 1995.
[20] Todoroki A., Haftka RT. "Lamination parameters for efficient genetic optimization of the stacking sequences of composite panels". *Proceedings of the 7th AIAA/USAF/NASA/ISSMOS Symposium on Multidisciplinary Analysis and Optimization*, St. Louis, USA, AIAA-1998-4816, pp 870-879, 1998.
[21] Narita Y., Hodgkinson JM. "Layerwise optimizations for maximising the fundamental frequencies of point-supported rectangular laminated composite plates". *Compos. Struct.*, 69, pp 127-135, 2005.
[22] Diaconu CG., Sekine H. "Layup optimization for buckling of laminated composite shells with restricted layer angles". *AIAA J.*, 42(10), pp 2153-2163, 2004.
[23] Todoroki A., Suenaga K., Shimamura Y. "Stacking sequence optimizations using modified global response surface in lamination parameters". *Adv. Compos. Mater.*, 12(1), pp 35-55, 2003.
[24] Todoroki A., Sasai M. "Stacking sequence optimizations using GA with zoomed response surface on lamination parameters". *Adv. Compos. Mater.*, 11(3): pp 299-318, 2003.
[25] Cheng S., Ho BPC.. "Stability of heterogeneous aeolotropic cylindrical shells under combined loading". *AIAA J.*, 1(4), pp 892-898, 1963.